galaxies

IMPACT FACTOR 3.8

CITESCORE 6.3

Article

ASKAP Detection of the Ultra-Long Spin Period Pulsar PSR J0901-4046

Emil Lenc, Philip G. Edwards, Susmita Sett and Manisha Caleb

Special Issue
Recent Advances in Radio Astronomy

Edited by
Dr. Phil Edwards

MDPI

https://doi.org/10.3390/galaxies13060131

galaxies

MDPI

Article

ASKAP Detection of the Ultra-Long Spin Period Pulsar PSR J0901−4046

Emil Lenc [1], Philip G. Edwards [1,*], Susmita Sett [2] and Manisha Caleb [3]

[1] CSIRO Space and Astronomy, Australia Telescope National Facility, Epping, NSW 1710, Australia; emil.lenc@csiro.au
[2] International Centre for Radio Astronomy Research, Curtin University, Perth, WA 6845, Australia; susmita.sett@curtin.edu.au
[3] Sydney Institute for Astronomy, School of Physics, The University of Sydney, Sydney, NSW 2006, Australia; manisha.caleb@sydney.edu.au
* Correspondence: philip.edwards@csiro.au

Abstract

A radio source with a period of 75.88 s, suspected of being an ultra-long period pulsar, was discovered in 2020 with the MeerKAT radio telescope. Here, we report the detection of radio pulses from this object in multi-epoch ASKAP image data at frequencies between 744 MHz and 1800 MHz and a search for pulses made in Murchison Widefield Array data at 154 MHz. The ASKAP detections pre-date and extend other published observations and so support the belief the pulsar emission has been persistent. The non-detection of the pulsar in MWA data is consistent with a recent report that the spectrum turns over at low frequencies. An ASKAP image of the field centred at 943 MHz confirms the MeerKAT detection of diffuse emission surrounding the pulsar.

Keywords: pulsars; neutron stars; radio continuum

Academic Editor: Dimitris M. Christodoulou

Received: 24 October 2025
Revised: 24 November 2025
Accepted: 28 November 2025
Published: 1 December 2025

Citation: Lenc, E.; Edwards, P.G.; Sett, S.; Caleb, M. ASKAP Detection of the Ultra-Long Spin Period Pulsar PSR J0901−4046. *Galaxies* **2025**, *13*, 131. https://doi.org/10.3390/galaxies13060131

1. Introduction

PSR J0901−4046 was discovered with the detection of a single pulse by the MeerTRAP project by Caleb et al. [1]. Further inspection of that data set, and subsequent observations, revealed a source with a period of 75.88 s. The measured dispersion measure of 52 ± 1 pc cm^{-3} suggests a distance of ∼0.4 kpc. Caleb et al. [1] also note the presence of a diffuse shell-like structure surrounding the PSR J0901−4046, though caution that more analysis is required to determine whether it is associated with the source. PSR J0901−4046 shares some properties with "normal" pulsars: (i) a steep spectral index, α, of -1.7 ± 0.9 (where $S \propto \nu^{\alpha}$), and (ii) a small duty cycle, with half-power pulse widths of ∼300 ms. It has no detectable X-ray emission but has other properties which more closely resemble those of magnetars, including (i) highly variable pulses, which can be classified into seven different pulse types (including the presence of a quasi-periodicity in some bright pulses), and (ii) a high surface magnetic field strength of 1.4×10^{14} G, assuming a dipolar magnetic field configuration.

The location of PSR J0901−4046 in the $P - \dot{P}$ diagram is however offset from both normal pulsars and magnetars, and so its classification is not yet clear [1]. This is primarily due to the unusually long period. The ATNF Pulsar Catalogue (http://www.atnf.csiro.au/research/pulsar/psrcat) [2] contains 4303 entries (as of 24 October 2025), with 65 of these being RRATs (Rotating Radio Transients) of unknown periods. Of the remaining 4238 pulsars, only 17 have periods longer than 10 s. Two of these have periods between

20 and 30 s, with the 76 s period of PSR J0901−4046 placing it at the extreme end of the population. (However, we note the recent discovery of a 41 s pulsar does start to bridge this gap [3].) The growing class of long-period radio transients have significantly longer periods, ranging from 18 min to several hours (e.g., [4–8]), and lie beyond the pulsar "death line" hinting that other emission mechanisms might be involved. However, the discovery of CHIME J0630+25 by Dong et al. [9] which has a period of 421 s, and with evidence for a timing glitch similar to that seen in some other pulsars, suggests that rotating neutron star models may be valid for periods even longer than that of PSR J0901−4046.

With such a long period, PSR J0901−4046 challenges the usual dipole spin-down model for pulsar evolution. Magnetic dipolar losses alone cannot readily explain such long spin periods and require extreme conditions like strong and long-lasting magnetic fields. Ronchi et al. [10] studied the spin evolution of young, isolated neutron stars under the influence of fallback accretion and demonstrate that the evolution of such an object can differ significantly from standard spin-down models, with neutron stars able to reach spin periods >10 s on timescales on the order of only 10^3∼10^5 years. Similarly, Gençali et al. [11] conclude that, as a result of fallback accretion, PSR J0901−4046, which is $\sim 7 \times 10^5$ years old, would have passed through an anomalous X-ray pulsar/soft gamma-ray repeater stage at an age of a few 10^4 years. The possibility of reaching such long spin periods in much less than 10^7 years is crucial to maintaining the magnetic field and thus an energy reservoir to power the object's radio or X-ray activity. Alternatively, Konar [12] propose an ultra-strong magnetic field anchored near the core–crust boundary as a solution to the apparent mystery of GLEAM-X J162759.5−523504.3, a long-period radio transient with a periodicity of 1091 s [5], and find that it scales well for PSR J0901−4046.

Several of the first long-period radio transients to be discovered were only active for short periods, from days to months (e.g., [4–6]). The MeerKAT discovery observations of PSR J0901−4046 spanned 17 September 2020 to 9 May 2021, and Caleb et al. [1] note that further information on how persistent the source is would provide further clues as to its nature. Subsequent observations between 2021 and 2023 by Bezuidenhout et al. [13] indicate that the source has continued to emit pulses and has not yet shown any evidence of being episodic.

Here, we report on observations of PSR J0901−4046, which both precede the original MeerKAT discovery and extend the Bezuidenhout et al. [13] monitoring, with the ASKAP radio telescope and the Murchison Widefield Array (MWA).

2. The Search for Pulses

2.1. ASKAP Observations

The Australia SKA Pathfinder is an array of thirty-six 12 m diameter antennas, each of which uses a 188-element Phased Array Feed to provide wide field-of-view imaging over a 288 MHz bandwidth in the 700 to 1800 MHz range [14]. The ASKAP correlator uses a cycle time of 9.953281 s, which we round to 10 s in the discussion below. Data are integrated over this cycle time with visibilities written to disk at the end of each cycle. Although the original MeerKAT pulses were only ∼300 ms wide, they were sometimes bright enough that it appeared worthwhile to examine the ASKAP data to see whether they were detectable in 10 s integrations. Caleb et al. [1] noted that the first Rapid ASKAP Continuum Survey (RACS) was not sensitive enough to detect a persistent source as the time-averaged flux of a couple of hundred micro-jansky lay below the median RMS image noise of 250 μJy beam^{-1} [15]. Examination of each 10 s integration individually, and folding the resulting data with the pulsar period, offered the possibility of detecting the pulsar, particularly if it happened to emit a bright pulse during a 10 s integration within a 15 min observation.

A series of RACSs have been undertaken to develop a global sky model, and streamline operational procedures, by imaging the visible sky using a 15 min integration for each pointing [15]. To date, three surveys in the ASKAP low (∼900 MHz) band have been made, two surveys in the mid (∼1300 MHz) band, and one survey in the high (∼1600 MHz) band.

The first RACS-low (retrospectively referred to as RACS-low1), centred at 888 MHz, was conducted in 2019, with a number of fields re-observed in 2020 [16]. A second epoch of RACS-low, RACS-low2, was undertaken in 2021/2022, with an improved sensitivity resulting from increases in system reliability and enhancements in data processing. Both RACS-low1 and RACS-low2 used the "square_6x6" beam footprint, which is detailed in [14]. A third epoch, RACS-low3, was completed in early 2024, using the more compact "closepack36" beam footprint (to match with RACS-mid and RACS-high) and a slightly higher frequency for better sensitivity.

The RACS-mid1 commenced in late 2020 [17,18]. As the bottom half of the 288 MHz bandwidth RACS-mid is significantly impacted by GNSS satellite signals, only the top half of the band was used, yielding an effective band centre of 1367 MHz. A second epoch, RACS-mid2, was conducted in 2024 with processing of this data still underway. The RACS-high survey, centred on 1655 MHz, followed in 2022 [19].

Inspired by promising early results, a 10 h test observation was made of the field which included PSR J0901−4046 in June 2022, and a 1 h ToO (Target of Opportunity) observation was made on 3 October 2025. Table 1 provides the list of ASKAP observations considered here. The columns give (1) the observing program; (2) the scheduling block identification, SBID; (3) the name of the observed field; (4) the beam number (see Hotan et al. [14] for the mapping of the beam number for the beam footprint); (5) the offset in degrees of the source from the beam centre; (6) the start time, corresponding to the first unflagged data (which can be 30∼40 s after the nominal start time of the observation); and (7) the frequency range. Details of the RACS data processing are given in McConnell et al. [15], Hale et al. [16], and Duchesne et al. [17–19].

Table 1. ASKAP Observing Log. RACS observations were all 15 min in duration, the test observation 10 h, and the ToO observation 1 h.

Survey	SBID	Field	Beam	Offset (deg)	Date (yyyy-mm-dd)	Start Time (UT)	Frequency Range (MHz)
RACS-low1_1	8598	RACS_0911-37A	30	0.62	2019-04-30	14:06:59.7	743.491–1031.491
RACS-low1_2	8641	RACS_0855-43A	20	0.69	2019-05-04	05:09:51.4	743.491–1031.491
RACS-low1_3	13739	RACS_0855-43A	20	0.69	2020-05-02	11:21:04.8	743.491–1031.491
RACS-mid1_1	22042	RACS_0859-41	27	0.08	2021-01-26	17:19:37.7	1151.491–1439.491 [a]
RACS-high1_1	35676	RACS_0859-41	27	0.08	2022-01-10	18:40:51.7	1511.491–1799.491
RACS-low2_1	39244	RACS_0911-37	30	0.62	2022-04-11	12:44:53.6	743.491–1031.491
RACS-low2_2	39310	RACS_0855-43	19	0.72	2022-04-12	12:13:30.8	743.491–1031.491
Test_0900-40	41912	TEST_0900-40	9	0.56	2022-06-25	01:23:34.4	799.491–1087.491
RACS-low3_1	56856	RACS_0859-41	27	0.08	2024-01-06	19:02:18.8	799.491–1087.491
RACS-mid2_1	67689	RACS_0859-41	27	0.08	2024-11-10	22:46:28.6	1151.491–1439.491 [a]
ToO	77422	PSR_J0901-4046	15	0.00	2025-10-03	22:37:51.6	799.491–1087.491

a: only top half of 288 MHz bandwidth used.

For our examination of each ten-second integration separately, the following steps were taken: (i) A model of the field was determined from the RACS-low2 and RACS-low3 catalogues and extrapolated to the central frequency of each observation using a spectral index of −0.83. The model is attenuated with a Gaussian approximation of the primary beam that takes into consideration the effect on the spectral index of each source depending on its position in relation to the centre of the beam. (ii) The visibilities are then bandpass-calibrated against the sky model. This ensures that phases are well calibrated and that

short time-scale images can be made. (iii) A frequency-independent amplitude and phase self-cal against the model was made to account for any time variability in the gains. (iv) The model is subtracted from the visibility data. This should leave behind only small residual components around field sources. (v) Small dirty images (no deconvolution is applied since most field source structure has been removed) are made using the CASA task tclean for each ASKAP integration, phase-shifted so that the image is centred on the location of the pulsar (to reduce non-co-planar effects). This allows for very fast imaging at short time-scales. (vi) The background image noise; the presence of any peak in the subtracted field; and the signal-to-noise ratio (SNR) of that peak are measured. We do not attempt to measure flux densities for the detected pulses as the (variable, see below) noise contribution would make a sizeable contribution to the error.

The results for nine RACS epochs are shown in Figure 1. Vertical grey lines indicate when a pulse would be expected based on the ephemeris given in [13]. Pink vertical lines indicate pulses exceeding an SNR level of typically 3.4 σ, corresponding to approximately a 1 in 1000 chance of a statistical fluctuation exceeding this level, indicated by the dotted horizontal line. As the distribution of SNR values is not a simple Gaussian and may vary from observation to observation depending on the calibration and how well the field is subtracted, the "significant" value adopted for each epoch followed inspection of the data to find a reasonable value.

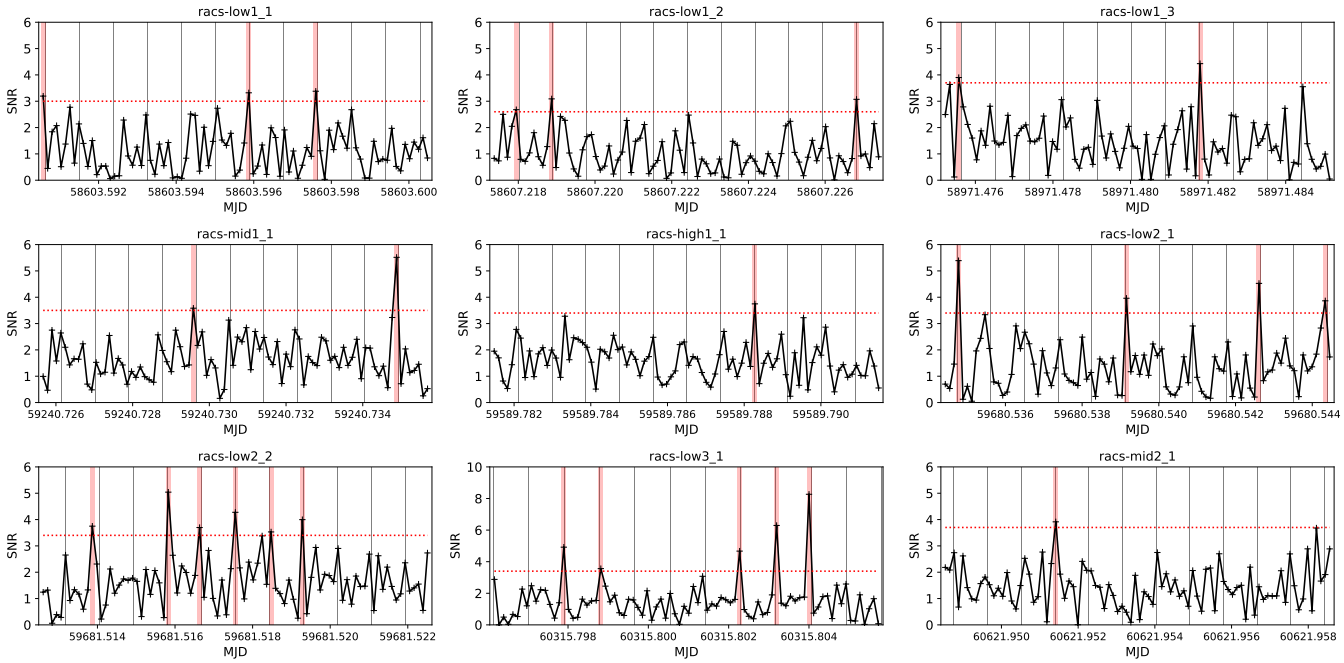

Figure 1. The signal-to-noise ratio (SNR) for the pixel centred on the pulsar for each 10 s integration in the RACS observations. Vertical pink lines denote 10 s integrations with a signal-to-noise ratio exceeding the threshold for that run (see text for details), which is indicated by the red dashed line. Vertical grey lines indicate the predicted pulse arrival times.

It is apparent from Figure 1 that pulses exceeding the adopted significance level are seen at all epochs and in all three survey bands. A total of 26 of the 27 pulses coincide with the predicted pulsar period. There are approximately 800 ten-second bins in total across all nine epochs, and so the detection of a single pulse not aligned with the pulsar period (in the RACS-low2_2 epoch) is consistent with random fluctuations. We have repeated this analysis for a pixel offset by (10,10) pixels in the image, where the pixel size is 2 $\times$ 2 arcs. This also resulted in a single pulse exceeding the nominal significance level, consistent with the expected false positive rate.

Although we are in the small number statistics regime, it is noteworthy that, generally, more pulses were detected in the later RACS_low observations, consistent with improvements in sensitivity with the array operations and processing. Only a single pulse was detected in the RACS_high band, consistent with the steep spectrum of the pulsar. Although the RACS-mid epochs used only half of the 288 MHz bandwidth, they are more sensitive than RACS-low1 and RACS-low2 as the ASKAP effective system temperature is lowest in this band (see Figure 22 of [14]), with the fewer pulses (three) consistent with the falling pulsar spectrum.

The 15 min RACS observations correspond to 12 pulsar periods. The 10 h test observation on June 2022 in contrast covered 474 periods. The plot of the SNR for each 10 s is shown in the top panel of Figure 2. In 129 instances (27%) a pulse above a 3.7σ limit was detected. All but one coincide with the predicted time bin. The bottom panel of Figure 2 shows the power spectrum for a range of trial frequencies. By far the most significant frequency bin is consistent with the pulsar period. The corresponding period, 75.528 s, does not match the 75.88 s pulsar period exactly as the ASKAP arrival times are quantised by the 10 s correlator cycle time.

It appears that the off-peak SNRs in Figure 2 are not distributed as randomly as might be expected—as illustrated by the clusters of elevated values around 0.30 and 0.35. Although the analysis used visibility data from which the field had effectively been subtracted, there are some complex sources in the complete 5° × 5° field of view which may not subtract perfectly as a result of the PSF rotating substantially between integrations. It is possible that some artefacts in the single-cycle point spread function are slowly drifting across the image.

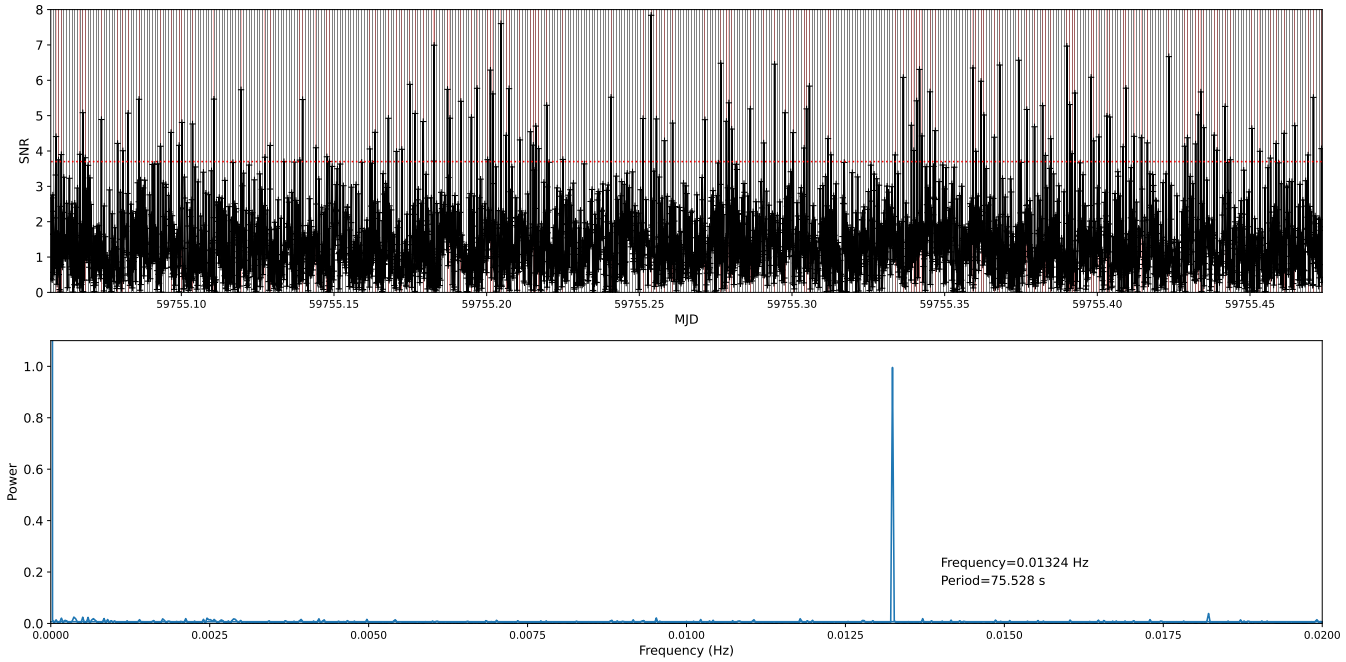

Figure 2. (**Top**) The SNR for the pixel centred on PSR J0901−4046 for each 10 s integration in the 10 h long observation in June 2022. Pink vertical lines indicate pulses above a 3.7σ significance (shown by the dashed red line), and grey vertical lines indicate expected pulse arrival times. (**Bottom**) The power spectrum for the pixel centred on the pulsar. By far the most significant power is seen at a value consistent with the pulsar period.

A comparison was made by repeating the analysis for a point offset by (10,10) pixels in the image. The result is shown in Figure 3. Only five peaks above the 3.7σ threshold are seen, and only two of these fall in the expected time bin. The overall trend of SNRs with

time still shows some low-level quasi-sinusoidal variability, which we again attribute to sidelobes slowly varying with time across the image.

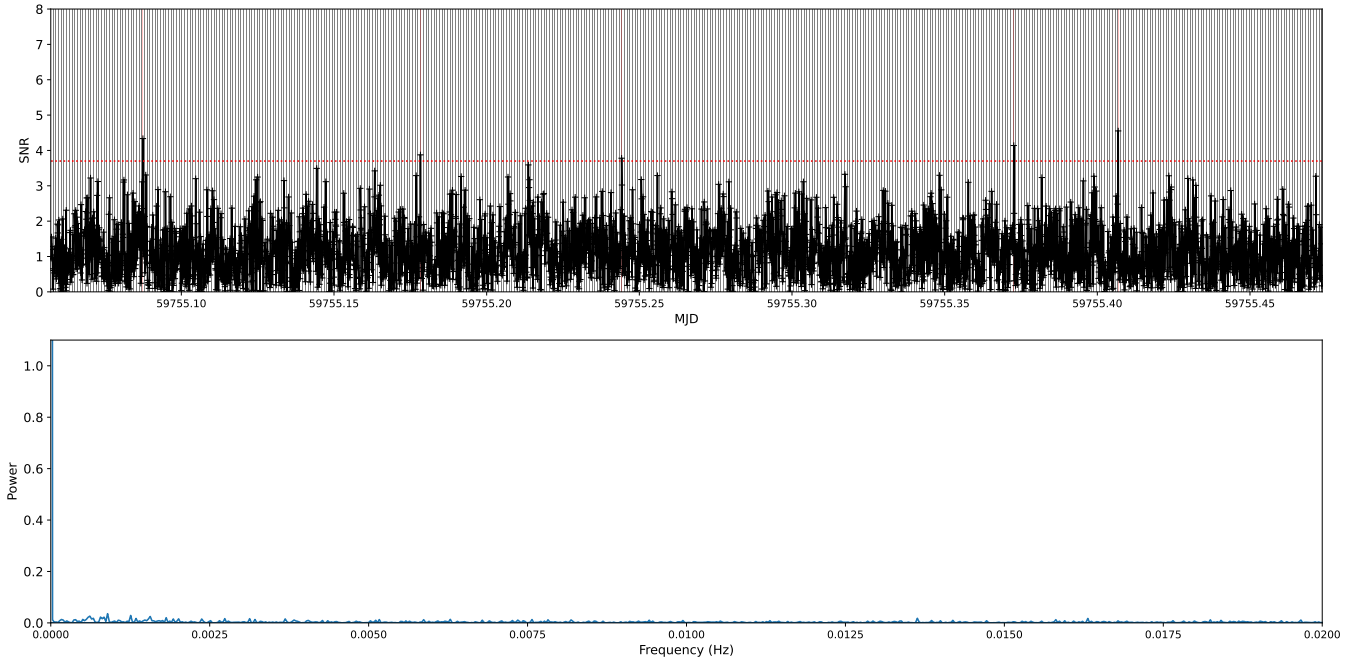

Figure 3. The same analysis as for Figure 2, for a pixel offset by (x,y) = (10,10) pixels from PSR J0901−4046.

As a final check of the stability of the pulsar ephemeris, a Target of Opportunity request was made for one more ASKAP epoch. A one-hour observation was conducted on 3 October 2025, with the results shown in Figure 4. Twenty-two pulses exceeding 3.4σ were detected, amounting to 46% of pulse periods, and all consistent with the 75.88 s period. (The next highest peak, with an SNR just below 3.4, did not fall at the expected bin.) For this observation a beam near the centre of the 6×6 beam footprint was used, with the pulsar located at the centre of the beam, and the improved sensitivity provided by these changes will have contributed to the significantly higher pulse detection percentage. For a point offset by (10,10) pixels, three pulses above the same significance were detected. Although less than one pulse exceeding 3.4σ would be expected purely by chance, this is the regime of small number statistics, and the false positive rate is much smaller than the true positive rate.

Although the pulse arrival times are quantised with the 10 s correlator integration time, we trialled determining a pulsar ephemeris from the ASKAP data alone. We used the `tempo2` (version 2024.04.1) software package [20] to derive a new ephemeris from all the ASKAP data presented in this paper, a data set spanning 2348.4 days (or 6.43 years). Using the arrival times of the 178 pulses above the significance level adopted for each run (and including the two pulses which did not coincide with the predicted bin), we obtained P = 75.8855481(9) s and $\dot{P} = 2.2(1) \times 10^{-13}$ for T0 = MJD 59,231, consistent with the ephemerides of [1,13]. This ephemeris has benefitted from the longer time range of the observations but is limited by the 10 s ASKAP integration time.

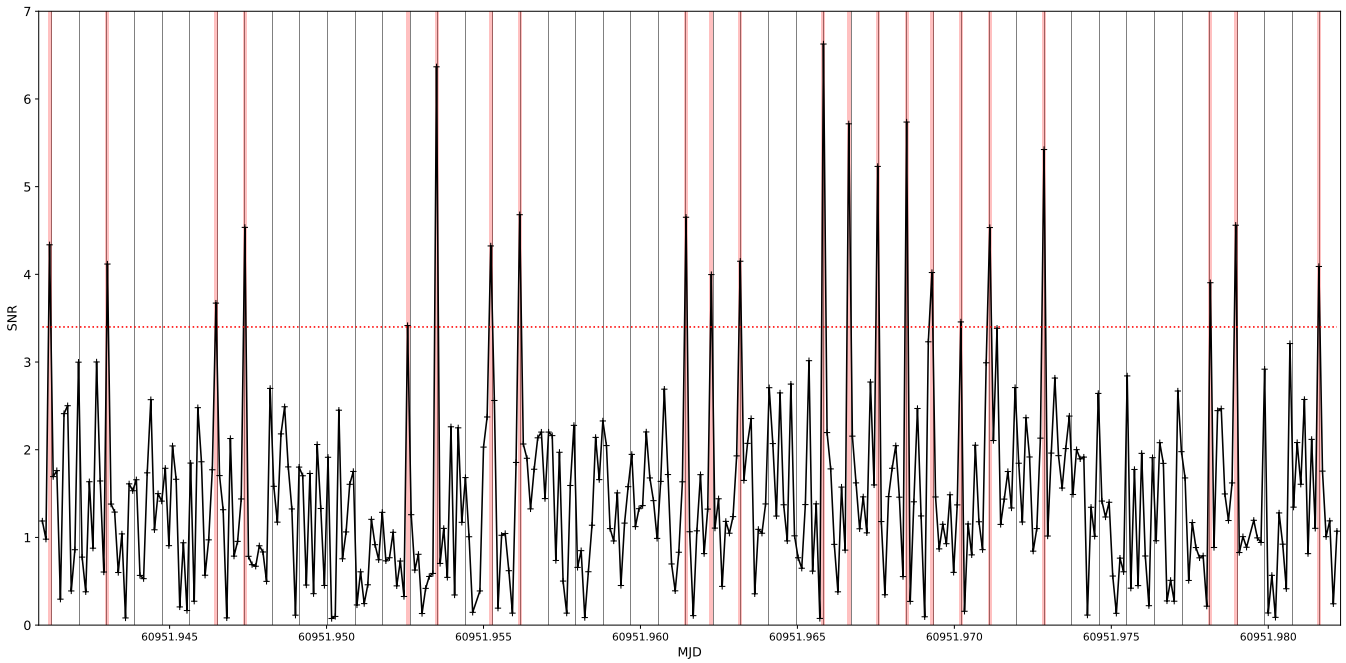

Figure 4. The SNR for the pixel centred on PSR J0901−4046 for each 10 s integration in the 1 h long Target of Opportunity observation in October 2025. Pink vertical lines indicate pulses above a 3.4σ significance (shown by the dashed red line), and grey vertical lines indicate expected pulse arrival times.

2.2. MWA Observation

The Murchison Widefield Array (MWA, [21–23]) is a low-frequency precursor telescope to the SKA-low telescope in Western Australia. It consists of 256 tiles, each of which has 16 dipole antennas laid out in a 4 × 4 grid. It operates in the frequency range of 70–300 MHz. This work uses MWA Phase II observations, in the extended array configuration, with a central observing frequency of 154 MHz and a bandwidth of 30 MHz, using 128 tiles. The MWA observation started 6 March 2018 at 14:18:05.5 UT, approximately 2.5 years before the MeerKAT discovery. Images were made every second of the ∼1 h observation; however, there is no evidence of the pulsar in data folded with the (extrapolated) pulsar period, or with a range of trial periods around that value. The binned light-curves had about 30 samples per bin and a sensitivity of ∼5 mJy/beam in each bin. Based on the MeerKAT spectral index of -1.9 ± 0.9, measured in the range 856 to 1712 MHz [1], a mean flux density of ∼500 mJy/beam might have been expected (assuming minimal pulse smearing), which would have been readily detectable. The fact that no pulses were detected implies that (a) the pulsar was not emitting pulses at that epoch, or (b) the spectrum flattens or turns over between the MeerKAT band and the MWA band, or (c) the pulse is significantly smeared or broadened at low frequencies. [13] have subsequently reported the results of observations with the MWA, GMRT, and MeerKAT. Pulses were detected in MeerKAT UHF-band observations (544 to 1088 MHz) and GMRT band 4 observations (550 to 750 MHz). However, no pulses were detected in GMRT band 3 (300 to 500 MHz) or a single epoch MWA observation made in March 2022. A turn-over in the spectrum below ∼500 MHz, as has been seen in some other pulsars, would appear likely [13].

3. ASKAP Imaging

The deepest MeerKAT image of the field shows a partially visible, diffuse shell-like structure surrounding PSR J0901−4046 [1]. While the possibility that this is the supernova remnant from the event that formed the neutron star is noted, Caleb et al. [1] caution that

the complexity of the diffuse emission in the field requires additional analysis to determine whether there is a robust association of the radio shell with PSR J0901−4046. Extended Data Figure 7 of [1] shows a 12 arcmin × 12 arcmin region centred on the pulsar, with an arc of diffuse emission evident ∼5 arcmin to the east.

A one-degree by one-degree ASKAP image from the 10 h observation in June 2022 and centred at 943 MHz is shown in Figure 5. The location and morphology of the diffuse emission to the east of the pulsar closely match that of the MeerKAT image. The wider field of view reveals further diffuse emission to the north and west of the pulsar. The extent of emission to the north, and orientation of the emission to the west, complicate the interpretation of the emission as a supernova remnant and highlight the complex nature of diffuse emission in this part of the galactic plane, $(l, b) = (263.1^\circ, 3.7^\circ)$. Further observations are required.

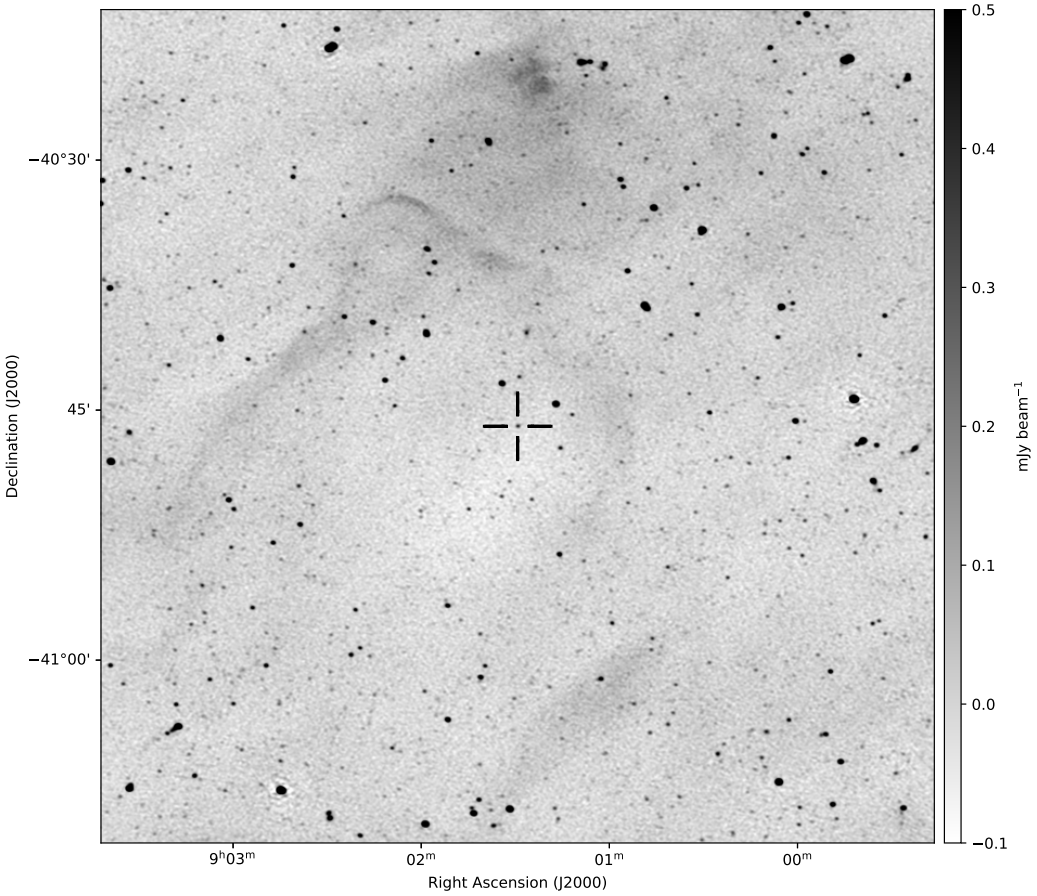

Figure 5. ASKAP image at 943 MHz of the field surrounding PSR J0901−4046, from the 10 h observation on 25 June 2022. The image is 46 arcmin across. The position of the pulsar (not detectable in individual 15 min RACS images but which is detectable in the 10 h run) is marked.

4. Conclusions

We have observed the ultra-long spin period pulsar PSR J0901−4046 with ASKAP at frequencies between 743 and 1799 MHz, at 11 epochs between April 2019 and October 2025, and with the MWA at 154 MHz in March 2018.

Although ASKAP data is integrated for 10 s before being written to disk, pulses exceeding $\sim 3.4\sigma$ are seen in the time bins predicted to include pulses from PSR J0901−4046 in all epochs. Caleb et al. [1] originally reported an apparent secular decline in averaged flux density over the 3 years of their observations, but the subsequent observations by Bezuidenhout et al. [13] indicate this trend did not continue. In contrast, the trend in

the ASKAP detections was for pulses to be detected more frequently with time (in the low-band); however, this can be ascribed to improvements in ASKAP calibration and processing and source location in the beam rather than any reflection of source behaviour. The earliest ASKAP observations precede the MeerKAT detection by 1.4 years, and the most recent ASKAP observation is two years after the last observation of Bezuidenhout et al. [13]. An ephemeris determined from the ASKAP pulses is consistent with those of Caleb et al. [1] and Bezuidenhout et al. [13] and confirms that the source's timing solution displays a remarkable stability [13].

The 10 h ASKAP observation in June 2022 yielded 129 pulses above 3.7σ, with a comparison pixel nearby suggesting only $\sim$5 pulses would be expected by chance. This long observation also allowed the field to be imaged, confirming both the detection by [1] of surrounding diffuse emission in the MeerKAT image and their caution in associating it with the pulsar.

The MWA observation in March 2018 — the earliest published observation of this field— did not detect any pulses from PSR J0901−4046. This is consistent with the subsequent non-detections by [13] and suggests a turn-over in, or flattening of, the spectrum below 500 MHz.

These observations have demonstrated the ability of ASKAP to contribute to studies of longer-period sources, even with very narrow duty cycles, despite its 10 s correlator cycle. The high time resolution CRACO system [24] recently deployed on ASKAP will enable studies of pulse profiles to also be pursued. Deeper radio imaging of the diffuse emission surrounding PSR J0901−4046 may enable the distance to be constrained through the presence of HI emission or absorption lines in the spectrum and determine whether it is consistent with the distance of $\sim$0.4 kpc derived from the Dispersion Measure of the pulsar. Multi-epoch astrometric VLBI observations could measure the proper motion of the pulsar and determine whether it is consistent with the scenario of some of the diffuse surrounding material being part of an associated supernova remnant. Ongoing studies will allow for the connection between ultra-long period pulsars and other long-period radio transients to be clarified.

Author Contributions: Conceptualisation, E.L. and P.G.E.; methodology, E.L.; analysis, E.L. and S.S.; investigation, E.L.; writing—original draft preparation, P.G.E.; writing—review and editing, P.G.E., E.L., S.S. and M.C. All authors have read and agreed to the published version of the manuscript.

Funding: This research received no external funding.

Data Availability Statement: ASKAP data products are made available through the CSIRO ASKAP Science Data Archive (CASDA; [25]—https://data.csiro.au/domain/casda). RACS data products are available under project code AS110, and data products from the test and ToO observations are available under project code AS113. MWA data is archived in a TAP (Table Access Protocol) service which can be assessed at http://vo.mwatelescope.org/mwa_asvo/tap.

Acknowledgments: We thank the anonymous referees for constructive comments that have improved the clarity of the paper. This scientific work uses data obtained from Inyarrimanha Ilgari Bundara, the Murchison Radio-astronomy Observatory. We acknowledge the Wajarri Yamaji People as the Traditional Owners and Native Title Holders of the Observatory site. The Australian SKA Pathfinder is part of the Australia Telescope National Facility (https://ror.org/05qajvd42) which is managed by CSIRO. Operation of ASKAP is funded by the Australian Government with support from the National Collaborative Research Infrastructure Strategy. Establishment of ASKAP, Inyarrimanha Ilgari Bundara, CSIRO's Murchison Radio-astronomy Observatory, and the Pawsey Supercomputing Research Centre are initiatives of the Australian Government, with support from the Government of Western Australia and the Science and Industry Endowment Fund. Support for the operation of the MWA is provided by the Australian Government (NCRIS), under a contract to Curtin University administered by Astronomy Australia Limited. S.S. would like to thank Ramesh Bhat and Marcin

Sokolowski for useful discussions and help with processing of the MWA data and interpretation of the results. George Hobbs, Beth Cappellazzo, and Lawrence Toomey are thanked for their interest and advice. This paper includes archived data obtained through the CSIRO ASKAP Science Data Archive, CASDA (http://data.csiro.au).

Conflicts of Interest: The authors declare no conflicts of interest.

Abbreviations

The following abbreviations are used in this manuscript:

ASKAP	Australian SKA Pathfinder
CASDA	CSIRO ASKAP Science Data Archive
CRACO	(ASKAP) CRAFT Coherent (system)
CRAFT	Commensal Realtime ASKAP Fast Transient
GMRT	Giant Metre-wave Radio Telescope
GNSS	Global Navigation Satellite System
MeerKAT	Meer Karoo Array Telescope
MWA	Murchison Widefield Array
RACS	Rapid ASKAP Continuum Survey
RRAT	Rotating Radio Transient
SNR	Signal-to-Noise Ratio
ToO	Target of Opportunity
UHF	Ultra-High Frequency

References

1. Caleb, M.; Heywood, I.; Rajwade, K.; Malenta, M.; Willem Stappers, B.; Barr, E.; Chen, W.; Morello, V.; Sanidas, S.; van den Eijnden, J.; et al. Discovery of a radio-emitting neutron star with an ultra-long spin period of 76 s. *Nat. Astron.* **2022**, *6*, 828–836. [CrossRef]
2. Manchester, R.N.; Hobbs, G.B.; Teoh, A.; Hobbs, M. The Australia Telescope National Facility Pulsar Catalogue. *Astron. J.* **2005**, *129*, 1993–2006. [CrossRef]
3. Wang, Y.; Uttarkar, P.A.; Shannon, R.M.; Lee, Y.W.J.; Dobie, D.; Wang, Z.; Bannister, K.W.; Caleb, M.; Deller, A.T.; Glowacki, M.; et al. The Discovery of a 41 s Radio Pulsar PSR J0311+1402 with ASKAP. *Astrophys. J. Lett.* **2025**, *982*, L53. [CrossRef]
4. Hyman, S.D.; Lazio, T.J.W.; Kassim, N.E.; Ray, P.S.; Markwardt, C.B.; Yusef-Zadeh, F. A powerful bursting radio source towards the Galactic Centre. *Nature* **2005**, *434*, 50–52. [CrossRef] [PubMed]
5. Hurley-Walker, N.; Zhang, X.; Bahramian, A.; McSweeney, S.J.; O'Doherty, T.N.; Hancock, P.J.; Morgan, J.S.; Anderson, G.E.; Heald, G.H.; Galvin, T.J. A radio transient with unusually slow periodic emission. *Nature* **2022**, *601*, 526–530. [CrossRef]
6. Caleb, M.; Lenc, E.; Kaplan, D.L.; Murphy, T.; Men, Y.P.; Shannon, R.M.; Ferrario, L.; Rajwade, K.M.; Clarke, T.E.; Giacintucci, S.; et al. An emission-state-switching radio transient with a 54-minute period. *Nat. Astron.* **2024**, *8*, 1159–1168. [CrossRef]
7. Lee, Y.W.J.; Caleb, M.; Murphy, T.; Lenc, E.; Kaplan, D.L.; Ferrario, L.; Wadiasingh, Z.; Anumarlapudi, A.; Hurley-Walker, N.; Karambelkar, V.; et al. The emission of interpulses by a 6.45-h-period coherent radio transient. *Nat. Astron.* **2025**, *9*, 393–405. [CrossRef]
8. Wang, Z.; Rea, N.; Bao, T.; Kaplan, D.L.; Lenc, E.; Wadiasingh, Z.; Hare, J.; Zic, A.; Anumarlapudi, A.; Bera, A.; et al. Detection of X-ray emission from a bright long-period radio transient. *Nature* **2025**, *642*, 583–586. [CrossRef]
9. Dong, F.A.; Clarke, T.E.; Curtin, A.; Kumar, A.; Mckinven, R.; Shin, K.; Stairs, I.; Brar, C.; Burdge, K.; Chatterjee, S.; et al. CHIME/Fast Radio Burst/Pulsar Discovery of a Nearby Long-period Radio Transient with a Timing Glitch. *Astrophys. J. Lett.* **2025**, *990*, L49. [CrossRef]
10. Ronchi, M.; Rea, N.; Graber, V.; Hurley-Walker, N. Long-period Pulsars as Possible Outcomes of Supernova Fallback Accretion. *Astrophys. J.* **2022**, *934*, 184. [CrossRef]
11. Gençali, A.A.; Ertan, Ü.; Alpar, M.A. Evolution of the long-period pulsar PSR J0901-4046. *Mon. Not. R. Astron. Soc. Lett.* **2023**, *520*, L11–L15. [CrossRef]
12. Konar, S. Enigma of GLEAM-X J162759.5–523504.3. *J. Astrophys. Astron.* **2023**, *44*, 1. [CrossRef]
13. Bezuidenhout, M.C.; Bhat, N.D.R.; Caleb, M.; Driessen, L.N.; Jankowski, F.; Kramer, M.; Morello, V.; Pastor-Marazuela, I.; Rajwade, K.; Roy, J.; et al. Slow and steady: Long-term evolution of the 76-s pulsar J0901-4046. *Mon. Not. R. Astron. Soc.* **2025**, *540*, 2131–2145. [CrossRef]

14. Hotan, A.W.; Bunton, J.D.; Chippendale, A.P.; Whiting, M.; Tuthill, J.; Moss, V.A.; McConnell, D.; Amy, S.W.; Huynh, M.T.; Allison, J.R.; et al. Australian square kilometre array pathfinder: I. system description. *Publ. Astron. Soc. Aust.* **2021**, *38*, e009. [CrossRef]
15. McConnell, D.; Hale, C.L.; Lenc, E.; Banfield, J.K.; Heald, G.; Hotan, A.W.; Leung, J.K.; Moss, V.A.; Murphy, T.; O'Brien, A.; et al. The Rapid ASKAP Continuum Survey I: Design and first results. *Publ. Astron. Soc. Aust.* **2020**, *37*, e048. [CrossRef]
16. Hale, C.L.; McConnell, D.; Thomson, A.J.M.; Lenc, E.; Heald, G.H.; Hotan, A.W.; Leung, J.K.; Moss, V.A.; Murphy, T.; Pritchard, J.; et al. The Rapid ASKAP Continuum Survey Paper II: First Stokes I Source Catalogue Data Release. *Publ. Astron. Soc. Aust.* **2021**, *38*, e058. [CrossRef]
17. Duchesne, S.W.; Thomson, A.J.M.; Pritchard, J.; Lenc, E.; Moss, V.A.; McConnell, D.; Wieringa, M.H.; Whiting, M.T.; Wang, Z.; Wang, Y.; et al. The Rapid ASKAP Continuum Survey IV: Continuum imaging at 1367.5 MHz and the first data release of RACS-mid. *Publ. Astron. Soc. Aust.* **2023**, *40*, e034. [CrossRef]
18. Duchesne, S.W.; Grundy, J.A.; Heald, G.H.; Lenc, E.; Leung, J.K.; McConnell, D.; Murphy, T.; Pritchard, J.; Rose, K.; Thomson, A.J.M.; et al. The Rapid ASKAP Continuum Survey V: Cataloguing the sky at 1 367.5 MHz and the second data release of RACS-mid. *Publ. Astron. Soc. Aust.* **2024**, *41*, e003. [CrossRef]
19. Duchesne, S.; Ross, K.; Thomson, A.J.M.; Lenc, E.; Murphy, T.; Galvin, T.J.; Hotan, A.W.; Moss, V.A.; Whiting, M.T. The Rapid ASKAP Continuum Survey (RACS) VI: The RACS-high 1655.5 MHz images and catalogue. *Publ. Astron. Soc. Aust.* **2025**, *42*, 38. [CrossRef]
20. Hobbs, G.B.; Edwards, R.T.; Manchester, R.N. TEMPO2, a new pulsar-timing package—I. An overview. *Mon. Not. R. Astron. Soc.* **2006**, *369*, 655–672. [CrossRef]
21. Tingay, S.J.; Goeke, R.; Bowman, J.D.; Emrich, D.; Ord, S.M.; Mitchell, D.A.; Morales, M.F.; Booler, T.; Crosse, B.; Wayth, R.B.; et al. The Murchison Widefield Array: The Square Kilometre Array Precursor at Low Radio Frequencies. *Publ. Astron. Soc. Aust.* **2013**, *30*, e007. [CrossRef]
22. Wayth, R.B.; Tingay, S.J.; Trott, C.M.; Emrich, D.; Johnston-Hollitt, M.; McKinley, B.; Gaensler, B.M.; Beardsley, A.P.; Booler, T.; Crosse, B.; et al. The Phase II Murchison Widefield Array: Design overview. *Publ. Astron. Soc. Aust.* **2018**, *35*, e033. [CrossRef]
23. Tingay, S.J. The Murchison Widefield Array Enters Adolescence: A Personal Review of the Early Years of Operations. *Galaxies* **2025**, *13*, 107. [CrossRef]
24. Wang, Z.; Bannister, K.W.; Gupta, V.; Deng, X.; Pilawa, M.; Tuthill, J.; Bunton, J.D.; Flynn, C.; Glowacki, M.; Jaini, A.; et al. The CRAFT coherent (CRACO) upgrade I: System description and results of the 110-ms radio transient pilot survey. *Publ. Astron. Soc. Aust.* **2025**, *42*, e005. [CrossRef]
25. Huynh, M.; Dempsey, J.; Whiting, M.T.; Ophel, M. The CSIRO ASKAP Science Data Archive. In *Proceedings of the Astronomical Data Analysis Software and Systems XXVII*; Ballester, P., Ibsen, J., Solar, M., Shortridge, K., Eds.; Astronomical Society of the Pacific Conference Series; Astronomical Society of the Pacific: San Francisco, CA, USA, 2020; Volume 522, p. 263.